Frustrated Tunnel Ionization of Noble Gas Dimers with Rydberg-Electron Shakeoff by Electron Charge Oscillation

A. von Veltheim,[1] B. Manschwetus,[2] W. Quan,[3] B. Borchers,[1] G. Steinmeyer,[1] H. Rottke,[1] and W. Sandner[1]
[1]*Max-Born-Institut für Nichtlineare Optik und Kurzzeitspektroskopie, Max-Born-Straße 2A, D-12489 Berlin, Germany*
[2]*CEA-Saclay, IRAMIS, Service des Photons, Atomes et Molécules, F-91191 Gif-sur-Yvette, France*
[3]*State Key Laboratory of Magnetic Resonance and Atomic and Molecular Physics,*
Wuhan Institute of Physics and Mathematics, Chinese Academy of Sciences, Wuhan 430071, China
(Received 18 September 2012; published 9 January 2013)

Strong field single ionization of homo- and heteronuclear noble gas dimers with ultrashort infrared laser pulses is experimentally investigated. A pronounced photoelectron yield maximum is found for dimers in the momentum range $|\mathbf{p}| \leq 0.1$ a.u. which is absent for the corresponding monomer. This yield enhancement can be attributed to a new two-step strong field ionization mechanism active only in the dimers. In the first step, frustrated tunnel ionization at one of the atomic centers populates Rydberg states, which then become ionized in a second step through charge oscillation within the dimer ion core.

DOI: 10.1103/PhysRevLett.110.023001 PACS numbers: 32.80.Rm, 32.80.Ee, 33.20.Xx, 33.80.Rv

Noble gas dimers are bound by weak polarization forces at a substantially larger internuclear separation than ordinary molecules are. This gives rise to a localization of the electrons at the two atomic centers. Photoionizing these species in a high intensity laser pulse is expected to open new ionization pathways differing from those of strongly bound molecules with delocalized valence electrons and from those typical for individual atoms [1–4]. On one hand, their photoionization is expected to approach the atomic limit. On the other hand, however, specific molecular aspects may turn out to prevail during or subsequent to strong field ionization or to excitation via, e.g., frustrated tunnel ionization (FTI) [5]. Characteristic molecular aspects may, e.g., manifest themselves in photoelectron spectra as interference phenomena due to the two identical photoelectron emission centers in homonuclear dimers. Alternatively, they may show up as secondary scattering of the photoelectron on the dimer ion core [1,6–8].

In this Letter we focus on a specific structure that we find in the photoelectron momentum distribution after strong field single ionization of noble gas dimers. A pronounced enhancement of the photoelectron yield, as compared to the electron yield from strong field ionization of the respective atomic constituent (monomer), appears at small electron momentum ($|\mathbf{p}| \leq 0.1$ a.u.). This structure is found to be characteristic for all homonuclear noble gas dimers (Ne_2, Ar_2, Kr_2, Xe_2). We are led to attribute this enhancement to a previously unreported two-step strong field ionization mechanism with the first step being FTI of the dimer. This step populates Rydberg states [5], which, in the monomer, are bound after the laser pulse is gone. These states can decay only via fluorescence, eventually to the atomic ground state or to metastable excited ones [5]. In the dimer the situation is different. Given that the electrons are well localized at the atomic constituents in the dimer ground state, FTI will excite one of the atoms with the dimer ion core charge initially localized at this atomic site. This excitation does not leave the ion core of the dimer in a time independent eigenstate. An electron charge oscillation will start in the core, also affecting the electron in the Rydberg state that was populated by FTI. One effect of the charge oscillation may be a shakeoff of the Rydberg electron into the ionization continuum.

The experiment has been done in a reaction microscope setup [9] (for more details see Ref. [1]). The noble gas dimers were formed in a supersonic expansion of either pure noble gases or mixtures of two of the latter, allowing the formation of mixed atom dimers. The stagnation pressure was optimized for the formation of the respective dimers, at the same time minimizing the formation of bigger clusters. Within the reaction microscope, the dimer beam crossed a Ti:sapphire laser beam at right angles in its focal spot. There, light intensities of up to $\approx 3 \times 10^{14}$ W/cm^2 were reached in pulses with a full width at half maximum of ≈ 25 fs. The ions and photoelectrons formed in the focal spot were extracted by a homogeneous electric field (field strength 478 V/m). After passing drift tubes, they were detected by microchannel plate detectors, which were equipped with position sensitive delay-line anodes. For each detected particle the time of flight and the impact position were measured, enabling the reconstruction of its momentum vector resulting from the photoionization process. In order to collect all photoelectrons, irrespective of their direction of emission, a homogeneous magnetic field was applied parallel to the electric extraction field (field strength 3.2 G).

For the case of small momentum, obvious differences between the photoelectron momentum distribution of the monomer and that of the corresponding homonuclear dimer are apparent in Fig. 1. The figure shows momentum distributions for strong field ionization of Ar [Fig. 1(a)] and Ar_2 [Fig. 1(b)]. The spectra were taken at a light intensity

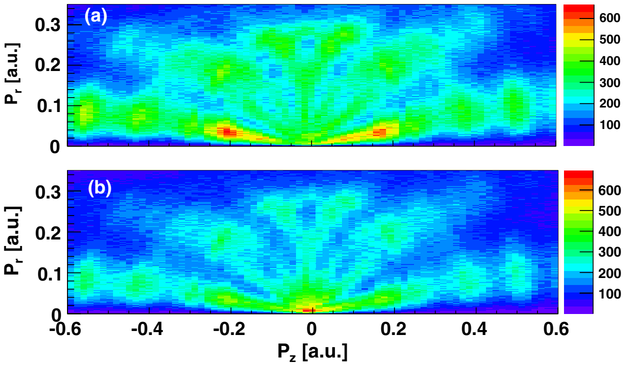

FIG. 1 (color online). Photoelectron momentum distributions after strong field single ionization of Ar atoms (a) and Ar_2 dimers (b).

of $\approx 2 \times 10^{14}$ W/cm^2 with the laser beam polarized linear along the p_z axis (abscissa in Fig. 1). The spectra are rotationally symmetric with respect to this axis. Thus, we plot the photoelectron yield using $p_r = (p_x^2 + p_y^2)^{1/2}$ as the ordinate. Only those photoelectrons detected together with Ar^+ [Fig. 1(a)] or Ar_2^+ ions [Fig. 1(b)] were included in the respective spectrum. Both spectra were taken in the same experimental run by sorting the photoelectrons using momentum conservation in the ionization process. A pronounced maximum in the Ar_2^+ spectrum, limited to a momentum range $|\mathbf{p}| \leq 0.1$ a.u., is visible. The same result is found for Ne_2 and Kr_2. For Xe_2 the yield enhancement is slightly more extended up to $|\mathbf{p}| \leq 0.15$ a.u.

The actual photoelectron yield enhancement can more easily be identified in a ratio spectrum $Y(Ar_2)/Y(Ar)$, which is calculated by bin-wise division of the yields in Figs. 1(a) and 1(b) and is shown in Fig. 2(a). A cut through this two-dimensional spectrum along the p_z axis with $p_r \in [0, 0.11$ a.u.$]$ [Fig. 2(b)] shows the enhancement quantitatively. The ratio was arbitrarily normalized to unity at $p_z = -0.6$ a.u. as absolute yield ratios are meaningless because of unknown detection efficiencies for Ar^+ and Ar_2^+ ions. Also included in Fig. 2(b) are the ratios found for Ne_2 and Kr_2. Figure 2(c) shows the analogous ratio spectra for the mixed atom dimers ArNe and ArKr by dividing the ArNe dimer spectrum by the Ar photoelectron spectrum and the ArKr spectrum by the Kr spectrum. Identical p_r cut intervals were chosen for all species. For each dimer the light intensity was chosen so as to avoid saturation of the ionization for the atomic constituent with the lowest ionization potential. The photoelectron yield enhancement appears for all homonuclear dimers, i.e., also for Xe_2 not shown here. It is also found for ArKr in the same p_z-momentum interval, however not for ArNe [Fig. 2(c)].

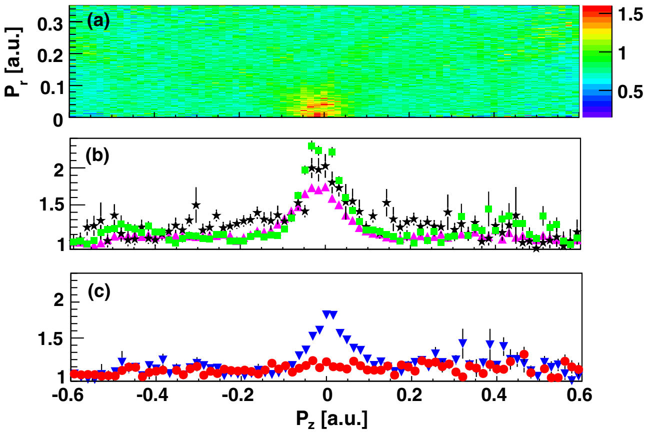

FIG. 2 (color online). (a) Ratio spectrum, $Y(Ar_2)/Y(Ar)$, obtained by bin-wise division of the photoelectron spectra from Fig. 1. (b) Projection of the ratio spectrum onto the p_z axis for $p_r \in [0, 0.11$ a.u.$]$: Ne_2 (black filled star), Ar_2 (magenta filled upward triangle), and Kr_2 (green filled square). (c) The analogous projections for ArNe (red filled circle) and ArKr (blue filled downward triangle).

The narrow momentum interval where the yield enhancement appears for the homonuclear dimers excludes interference through two-identical-center photoelectron emission as the origin of the yield enhancement, as already discussed in Ref. [1]. For dimers not aligned with respect to the polarization axis of the laser beam (as is the case in our experiment), one would expect the interference-based enhancement to extend over a momentum interval $|p_z|R \leq 1.2\pi$, where R is the equilibrium separation of the two atoms in the neutral dimer (see Ref. [1]). At this internuclear separation R the strong field ionization happens, and any nuclear dynamics is still frozen while the laser pulse is applied. For the dimers, R ranges between 5.9 a.u. (Ne_2) and 8.3 a.u. (Xe_2) [10,11]. Any interference enhancement is therefore expected to extend to $|p_z| \approx 0.45$ a.u. (Xe_2) or $|p_z| \approx 0.64$ a.u. (Ne_2). The fact that the yield enhancement is also present for ArKr dimers confirms this conclusion. Differing electron emission centers exclude two-center interference from appearing.

An alternative mechanism, internal scattering of the photoelectron wave, leaving one of the atomic sites after strong field ionization on the neighboring atom, may be held responsible for the local photoelectron yield enhancement at $|\mathbf{p}| = 0$. In this case two photoelectron waves would interfere on the photoelectron detector, i.e., one directly impinging on the detector and a scattered one. This interference phenomenon is known from x-ray photoionization of molecules and from charged particle scattering off molecules [12–14]. Recently, an equivalent interference effect has also been observed in strong field ionization of an atom [8]. Omitting small terms of order $(|f|/R)^2$ and any effect of the strong applied field on the continuum electron, the effect of internal scattering on the detector can be approximated for an unaligned dimer ensemble by

$$1 + 2\frac{|f|}{R}\frac{\sin|\mathbf{p}|R}{|\mathbf{p}|R}\cos(|\mathbf{p}|R + \chi_f), \qquad (1)$$

with $f = |f|\exp(i\chi_f)$ being the complex scattering amplitude, here for simplicity assumed to be isotropic, and R the internuclear separation. Depending on χ_f, the interference term in (1) may develop quite a narrow maximum at $|\mathbf{p}| = 0$. All dimers investigated should show this interference phenomenon, specifically also the mixed atom dimers. For ArKr, we actually find an enhancement near $|\mathbf{p}| = 0$. However, ArNe shows a flat photoelectron yield ratio at $|\mathbf{p}| = 0$. We may thus also exclude this kind of interference phenomenon as the origin of the yield ratio enhancement.

With the most obvious interference phenomena excluded that mainly distinguish noble gas dimer from monomer strong field ionization, we resort to a different excitation-ionization mechanism as a possible origin of the observed photoelectron yield enhancement. This two-step mechanism starts with FTI, causing the population of Rydberg states. The ionization of these states is then assumed to be induced by a secondary ionization mechanism that is common to all homonuclear and partially also to mixed noble gas dimers, yet impossible for monomers. The charge oscillation in the ion core of the Rydberg dimer, as introduced above, is such a secondary mechanism.

FTI of a homonuclear dimer leaves an electron in a Rydberg wave packet. At the same time, the pulse launches an electronic wave packet in the ion core, as all homonuclear dimer ions have two pairs of closely lying charge resonance states at the equilibrium internuclear separation of the neutral dimer, which serve as ionization thresholds [15]. Given their narrow spacing, all of these ionic states get excited at non-negligible probability. The resulting wave packet induces an electronic ion core charge oscillation between the two nuclear sites of the dimer, with its oscillation period determined by the energy separation of the participating pairs of charge resonance states. Via Coulomb interaction, this charge oscillation couples to the Rydberg electron and may induce its transition into the ionization continuum. Efficient ionization of the states making up the Rydberg wave packet is expected, provided that the ion core charge oscillation contains frequency contributions larger than the binding energy of the corresponding Rydberg state. Depending on the energy separation of charge resonance state pairs, this may happen only after the internuclear separation has decreased to values smaller than the neutral dimer equilibrium internuclear separation.

This two-step ionization scenario may also act in the heteronuclear dimers as evidenced by the ArKr case [Fig. 2(b)]. At the light intensity used, FTI may occur not only at the Kr but also at the Ar center of the dimer, as Ar and Kr ionization potentials differ by only ≈ 1.76 eV. For the ion core of the Rydberg dimer, this means that pairs of charge transfer dimer eigenstates become excited. Similar to the homonuclear dimers, therefore, a charge oscillation in the ArKr^+ ion core starts after FTI with the possibility of a shakeoff of the Rydberg electron. In ArNe the light intensity was chosen so as to only enable FTI of the Ar atom. The vast energy difference between the Ar and Ne ionization thresholds of 5.8 eV allowed reaching this regime. ArNe Rydberg states based on an excited $\mathrm{Ar\text{-}Ne}^+$ charge transfer ion core state are only found well above the Ar atom ionization threshold. As these states were inaccessible, the ion core charge of the excited ArNe remained localized at the Ar atom, and we find no photoelectron yield enhancement at $|\mathbf{p}| = 0$ [Fig. 2(c)]. The proposed two-step ionization mechanism is thus able to account for a yield enhancement we observed for ArKr and its absence for ArNe. It, however, remains to be shown that it actually may give rise to low energy photoelectrons.

The Rydberg state ionization mechanism introduced here is closely related to a mechanism well known from slow, close collisions between Rydberg- and ground-state atoms as associative- or chemi-ionization induced by a dipole resonance [16–21]. This mechanism was also assumed to give rise to autoionization found after noble gas dimer single photon excitation [22] and to low energy photoelectrons observed after dimer autoionization [23,24]. The latter would corroborate our enhanced detection of slow photoelectrons.

In order to get access to the momentum distribution of the shaken-off electron, we resort to a simplified, time dependent model to describe the Rydberg-electron dynamics after FTI populated Rydberg states. The Hamiltonian employed is (atomic units assumed)

$$H(t) = \frac{\mathbf{p}^2}{2} - \frac{Q(t)}{|\mathbf{x}|} - \frac{1 - Q(t)}{|\mathbf{x} - \mathbf{R}|}, \tag{2}$$

with $Q(t) = \cos^2(\Omega t/2)$. The charge oscillation is thus mimicked by a periodic transfer of charge between the two atomic centers of a dimer assumed to be located at $\mathbf{x} = \mathbf{0}$ and at $\mathbf{x} = \mathbf{R}$ at a frequency Ω. The interaction of the charge oscillation with the Rydberg electron is via simple Coulomb potentials. We start the motion of the Rydberg electron in the time dependent two-center Coulomb potential at $t = 0$ when the positive charge of the ion core is completely located at $\mathbf{x} = \mathbf{0}$. This assumes FTI having excited the atom located at $\mathbf{x} = \mathbf{0}$ and having left the electron in a Rydberg state $\phi_{n\ell m}(\mathbf{x})$ of this atomic constituent of the dimer at time $t = 0$. The initial Rydberg state is characterized by the principal, angular momentum, and magnetic quantum numbers, i.e., n, ℓ, and m, respectively. Since the laser polarization is linear and assumed here to be directed along the z axis, the magnetic quantum number m of the Rydberg state has to vanish ($m = 0$). In order to keep the calculation simple, we assume that the electron moves in a superposition of pure Coulomb potentials, thus ignoring short-range contributions to the potential, which are certainly present in noble gas atoms. In view of these considerations we rewrite the Hamiltonian (2) in the form $H = H_0 + V$ with H_0 and V given by

$$H_0 = \frac{\mathbf{p}^2}{2} - \frac{1}{|\mathbf{x}|}, \tag{3}$$

$$V(\mathbf{x}, t) = \left[\frac{1}{|\mathbf{x}|} - \frac{1}{|\mathbf{x} - \mathbf{R}|}\right][1 - Q(t)]. \tag{4}$$

At $t = 0$ the electron is thus in a Rydberg eigenstate of H_0, and we will calculate the transition rate into the ionization continuum of H_0 with the charge oscillation represented by $V(\mathbf{x}, t)$ as a time dependent perturbation of H_0.

Resorting to lowest order time dependent perturbation theory, the ionization rate of the dimer initially in a state $\phi_{n\ell 0}$ is then given by

$$W^{n\ell 0}_{p\ell' m'}(\mathbf{R}) = \frac{\pi}{8}\left|\left\langle \phi_{p\ell' m'} \left| \frac{1}{|\mathbf{x}|} - \frac{1}{|\mathbf{x} - \mathbf{R}|} \right| \phi_{n\ell 0} \right\rangle\right|^2, \tag{5}$$

with p the absolute value of the momentum of the shakenoff electron, ℓ' its angular momentum, and m' the magnetic quantum number. In the experiment $\mathbf{R}$ is statistically aligned with respect to the polarization vector of the laser pulse. It is thus necessary to average over all possible directions $\hat{\mathbf{R}} = \mathbf{R}/|\mathbf{R}|$ to obtain the actual ionization rate. For a Rydberg electron characterized by the quantum numbers n and ℓ, the ionization rate is then given by

$$\bar{W}^{n\ell}_p(R) = \sum_{\ell'=0}^{\ell'_{\max}} \sum_{m'=-\ell'}^{\ell'} \frac{1}{4\pi} \int d^2\hat{\mathbf{R}}\, W^{n\ell 0}_{p\ell' m'}(\mathbf{R}). \tag{6}$$

We sum over all possible final state magnetic quantum numbers m' and angular momentum quantum numbers ℓ' up to some $\ell'_{\max}$, where $W^{n\ell 0}_{p\ell' m'}$ becomes negligible. For given n and ℓ, the by far highest rate contributing to the sum over ℓ' is found for $\ell' = \ell + 1$. Moreover, the dipole contribution in a power series expansion of $V(\mathbf{x}, t)$ [Eq. (4)] with respect to $\mathbf{R}/|\mathbf{x}|$ mainly fixes the value of $\bar{W}^{n\ell}_p$. It is this very contribution which has always been used exclusively to determine associative ionization rates [16–21].

The dependence of the ionization rate [Eq. (6)] on the final momentum p of the continuum electron is shown for representative Rydberg states with principal quantum numbers $n = 8$, 16 in Fig. 3. $n = 8$ was chosen since there the excitation through FTI is expected to maximize [5]. The rate significantly differs from zero only for small values of p, and it increases significantly with decreasing ℓ. The range with a nonvanishing rate narrows with increasing ℓ, to $p < 0.25$ a.u. for $\ell \geq 5$ in the example. A similar behavior is found for any principal quantum number $n \gtrsim 5$ (see the $n = 16$, $\ell = 7$ result in Fig. 3) where the main population through FTI is expected to build up [5]. Independent of n the momentum range with a significant ionization rate is determined practically only by ℓ.

The outcome of the model combined with our experimental result has several tentative implications on the FTI of the dimers. Namely, FTI preferentially populates Rydberg states with high angular momentum ℓ. Only high ℓ states can give rise to the observed narrow, $p \lesssim 0.1$ a.u., enhancement of the photoelectron yield for dimers. ℓ has to be larger than approximately 7 to qualify. In turn, this means that the principal quantum numbers of the states populated have to be larger than approximately 8. The latter result is in tentative agreement with numerical calculations, however, for He atoms [5]. The condition for ℓ is presumably quite strict since the shakeoff rate increases significantly with decreasing ℓ (Fig. 3). In the experiment Rydberg states with low ℓ, if populated, would have preferentially contributed to the dimer spectrum with an electron yield enhancement extending beyond $p = 0.1$ a.u. (Fig. 3).

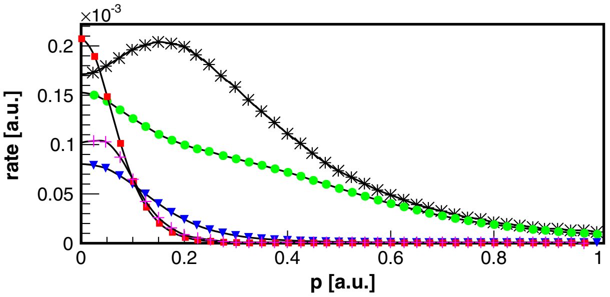

FIG. 3 (color online). The ionization rate (atomic units) induced by dimer ion core charge oscillation for $n = 8$ Rydberg states with angular momenta $\ell = 1$ (green filled circle), $\ell = 3$ (black asterisk), $\ell = 5$ (blue filled downward triangle), and $\ell = 7$ (red filled square), and for $n = 16$, $l = 7$ (magenta plus symbol). The internuclear separation was chosen to be that of Ar_2 ($R = 7.1$ a.u.). The $\ell = 7$ ($n = 8$, 16) rates are scaled by a factor of 20.

Summarizing, we have evidence of a new two-step strong field ionization mechanism, consisting of FTI with subsequent shakeoff of the Rydberg electron by dimer ion core charge oscillation. This mechanism is active in all noble gas dimers, provided that FTI populates coherently pairs of charge-resonance or charge-transfer ion core states. We expect this two-step mechanism to occur in any diatomic molecule at large internuclear separation when the electrons of the neutral molecule start to localize at the atomic cores, under the only constraint that the ionization potentials of the atomic constituents do not differ too much. Apart from dimers, this mechanism will potentially also be active in larger noble gas clusters which allow charge oscillation or migration over the cluster ion core.

We gratefully acknowledge funding by the Deutsche Forschungsgemeinschaft (DFG) and we thank H. Schmidt-Böcking (Institut für Kernphysik, Universität Frankfurt) for supporting us with the data acquisition.

---

[1] Z. Ansari, M. Böttcher, B. Manschwetus, H. Rottke, W. Sandner, A. Verhoef, M. Lezius, G. G. Paulus, A. Saenz, and D. B. Milošević, New J. Phys. **10**, 093027 (2008).
[2] B. Ulrich, A. Vredenborg, A. Malakzadeh, M. Meckel, K. Cole, M. Smolarski, Z. Chang, T. Jahnke, and R. Dörner, Phys. Rev. A **82**, 013412 (2010).

[3] B. Manschwetus, H. Rottke, G. Steinmeyer, L. Foucar, A. Czasch, H. Schmidt-Böcking, and W. Sandner, Phys. Rev. A **82**, 013413 (2010).

[4] J. Wu, A. Vredenborg, B. Ulrich, L. P. H. Schmidt, M. Meckel, S. Voss, H. Sann, H. Kim, T. Jahnke, and R. Dörner, Phys. Rev. Lett. **107**, 043003 (2011).

[5] T. Nubbemeyer, K. Gorling, A. Saenz, U. Eichmann, and W. Sandner, Phys. Rev. Lett. **101**, 233001 (2008).

[6] M. Busuladžić, A. Gazibegović-Busuladžić, D. B. Milošević, and W. Becker, Phys. Rev. A **78**, 033412 (2008).

[7] M. Okunishi, R. Itaya, K. Shimada, G. Prümper, K. Ueda, M. Busuladžić, A. Gazibegović-Busuladžić, D. B. Milošević, and W. Becker, Phys. Rev. Lett. **103**, 043001 (2009).

[8] Y. Huismans *et al.*, Science **331**, 61 (2011).

[9] J. Ullrich, R. Moshammer, A. Dorn, R. Dörner, L. P. H. Schmidt, and H. Schmidt-Böcking, Rep. Prog. Phys. **66**, 1463 (2003).

[10] J. M. Farrar, Y. T. Lee, V. V. Goldman, and M. L. Klein, Chem. Phys. Lett. **19**, 359 (1973).

[11] P. Slavícek, R. Kalus, P. Paska, I. Odvárková, P. Hobza, and A. Malievský, J. Chem. Phys. **119**, 2102 (2003).

[12] A. Landers, T. Weber, I. Ali, A. Cassimi, M. Hattass, O. Jagutzki, A. Nauert, T. Osipov, A. Staudte, M. H. Prior, H. Schmidt-Böcking, C. L. Cocke, and R. Dörner, Phys. Rev. Lett. **87**, 013002 (2001).

[13] X.-J. Liu, G. Prümper, F. Gel'mukhanov, N. A. Cherepkov, H. Tanaka, and K. Ueda, J. Electron Spectrosc. Relat. Phenom. **156–158**, 73 (2007).

[14] N. Stolterfoht, B. Sulik, B. Skogvall, J. Y. Chesnel, F. Frémont, D. Hennecart, A. Cassimi, L. Adoui, S. Hossain, and J. A. Tanis, Phys. Rev. A **69**, 012701 (2004).

[15] W. R. Wadt, J. Chem. Phys. **68**, 402 (1978).

[16] R. K. Janev and A. A. Mihajlov, Phys. Rev. A **20**, 1890 (1979).

[17] R. K. Janev and A. A. Mihajlov, Phys. Rev. A **21**, 819 (1980).

[18] L. M. Ignjatović and A. A. Mihajlov, Phys. Rev. A **72**, 022715 (2005).

[19] K. Miculis, I. I. Beterov, N. N. Bezuglov, I. I. Ryabtsev, D. B. Tretyakov, A. Ekers, and A. N. Klucharev, J. Phys. B **38**, 1811 (2005).

[20] J. Boulmer, R. Bonanno, and J. Weiner, J. Phys. B **16**, 3015 (1983).

[21] A. A. Mihajlov, V. A. Srećković, L. M. Ignjatović, and A. N. Klyucharev, J. Cluster Sci. **23**, 47 (2012).

[22] C. Y. Ng, P. W. Tiedemann, B. H. Mahan, and Y. T. Lee, J. Chem. Phys. **66**, 5737 (1977).

[23] X. K. Hu, J. B. A. Mitchell, and R. H. Lipson, Phys. Rev. A **62**, 052712 (2000).

[24] R. H. Lipson, X. K. Hu, J. B. A. Mitchell, and C. Froese-Fischer, Phys. Rev. A **68**, 012717 (2003).